

bradscholars

Tracing the architecture of caffeic acid phenethyl ester cocrystals: studies on crystal structure, solubility, and bioavailability implications

Item Type	Article
Authors	Ketkar, S.S.;Pagire, Sudhir K.;Goud, N.R.;Mahadik, K.R.;Nangia, A.;Paradkar, Anant R
Citation	Ketkar S, Pagire SK, Goud RN et al. (2016) Tracing the architecture of caffeic acid phenethyl ester cocrystals: studies on crystal structure, solubility, and bioavailability implications. Crystal Growth and Design. 16(10): 5710-5716.
DOI	https://doi.org/ 10.1021/acs.cgd.6b00759
Rights	This document is the Accepted Manuscript version of a Published Work that appeared in final form in Crystal Growth and Design, copyright © American Chemical Society after peer review and technical editing by the publisher. To access the final edited and published work see http://dx.doi.org/ 10.1021/acs.cgd.6b00759
Download date	2025-04-23 11:09:43
Link to Item	http://hdl.handle.net/10454/8911

The University of Bradford Institutional Repository

<http://bradscholars.brad.ac.uk>

This work is made available online in accordance with publisher policies. Please refer to the repository record for this item and our Policy Document available from the repository home page for further information.

To see the final version of this work please visit the publisher's website. Access to the published online version may require a subscription.

Link to publisher's version: <http://dx.doi.org/10.1021/acs.cgd.6b00759>

Citation: Ketkar S, Pagire SK, Goud RN et al. (2016) Tracing the architecture of caffeic acid phenethyl ester cocrystals: studies on crystal structure, solubility, and bioavailability implications. *Crystal Growth and Design*. 16(10): 5710-5716.

Copyright statement: This document is the Accepted Manuscript version of a Published Work that appeared in final form in *Crystal Growth and Design*, copyright © American Chemical Society after peer review and technical editing by the publisher. To access the final edited and published work see <http://dx.doi.org/10.1021/acs.cgd.6b00759>

Tracing the architecture of Caffeic acid phenethyl ester cocrystals: Studies on crystal structure, solubility and bioavailability implications

Sameer Ketkar[†], Sudhir K.Pagire[‡], N. Rajesh Goud[‡], KakasahebMahadik[‡], AshwiniNangia^{‡,¶} and AnantParadkar^{‡*}*

[†] Centre for Advanced Research in Pharmaceutical Sciences, Poona College of Pharmacy, BharatiVidyapeeth University, Pune-411038, India

[‡] Centre for Pharmaceutical Engineering Science, University of Bradford, Bradford, BD7 1DP, UK

[‡] School of Chemistry, University of Hyderabad, Prof. C. R. Rao Road, Gachibowli, Hyderabad, 500 046, India.

[¶]CSIR-National Chemical Laboratory, Dr. HomiBhabha Road, Pune 411 008, India.

ABSTRACT

Caffeic acid phenethyl ester (CAPE) is a polyphenolic active compound present in popular apipproduct, ‘propolis’ obtained from beehives. Though it has broad therapeutic capability, the bioavailability of CAPE is limited due to poor solubility. In this study, we report novel cocrystals of CAPE engineered using cofomers such as caffeine (CAF), isonicotinamide (INIC), nicotinamide (NIC) with enhanced solubility and bioavailability of CAPE. The cocrystals were prepared by microwave-assisted cocrystallization and characterized using PXRD, DSC and Raman spectroscopy. PXRD and DSC confirm the successful formation and phase purity of CAPE-CAF, CAPE-INIC and CAPE-NIC cocrystals. Raman spectra of CAPE cocrystals complement these results in confirming the formation of novel crystalline phases. CAPE-NIC cocrystal was further subjected to X-ray crystallography to understand its molecular arrangement and hydrogen bonding in the crystal structure. The CAPE-NIC cocrystal structure is found to be stabilized by a rare 1,2-benzenediol-amide heterosynthon. Cocrystallization of CAPE with NIC improved its aqueous solubility and pharmacokinetic profile thereby demonstrating 2.76 folds escalation in bioavailability.

1. Introduction

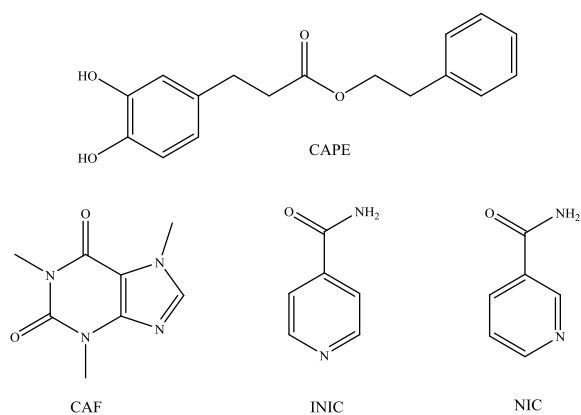
Polyphenolic compounds either synthetic or obtained from natural sources play an important role in therapeutic and nutritional applications.^{1,2,3} They are known to exhibit diverse pharmacological effects such as antioxidant, antimicrobial, anti-inflammatory, anticancer, antiviral, immunomodulatory, etc.^{4,5,6,7} Despite broad therapeutic utility, the poor aqueous solubility of polyphenols limits their bioavailability and makes their clinical efficacy questionable.^{1,2,8} Therefore, improving the physicochemical properties of polyphenols forms a

major focus of research worldwide. Pharmaceutical cocrystallization is a process by which a drug molecule and a coformer are brought together into the same crystal lattice to prepare novel solid forms of APIs with tailored physicochemical properties. This method has been successfully adapted to modulate the solubility of various polyphenolics. For example, the solubility and dissolution rate of curcumin and myricetin were improved by cocrystallizing with suitable coformers.^{9, 10} Further, cocrystallization was found to be advantageous in altering the pharmacokinetic profile of polyphenolics such as quercetin and epigallocatechin-3-gallate.^{11, 12} Binary solid composites, e.g. amorphous solid dispersions and eutectics are complementary strategies to improve the solubility of polyphenolics.^{13, 14, 15}

Caffeic acid phenethyl ester (CAPE) is a polyphenolic active present in popular apiproducpropolis, obtained from bee hives. CAPE is known to possess a wide array of pharmacological activities such as antioxidant, anti-inflammatory, antitumor, antibacterial, antiviral, neuroprotective, hepatoprotective, cardioprotective and immunostimulant.¹⁶⁻²³

Although numerous preclinical studies demonstrate the effectiveness of CAPE, its therapeutic utility is limited on account of its poor bioavailability which is ascribed to its poor aqueous solubility.^{24, 25} Most of the documented scientific reports focus on chemical synthesis^{26, 27, 28} and biological evaluation of CAPE or its derivatives.^{29, 16} However, a systematic analysis of its crystal structures directed towards improving its physicochemical properties is not known in the literature. A benzene solvate of CAPE is reported,³⁰ but its structural details were not found in the Cambridge Structural Database (CSD). Thus, till date there are no X-ray crystal structures on crystal forms of CAPE, either as single or multicomponent forms. The current study explores novel cocrystals of CAPE directed towards modulating its physicochemical properties. The microwave assisted cocrystallization³¹ technique was used to screen CAPE with various GRAS

(Generally Regarded As Safe) listed cofomers. In this study, we have found three novel cocrystals of CAPE with caffeine (CAF), isonicotinamide (INIC) and nicotinamide (NIC). The generation of novel crystalline forms of CAPE and understanding their structure-property relationships with special emphasis on improving its poor solubility and bioavailability forms the major focus of this article.



Scheme 1. Chemical structures of CAPE and cofomers.

2. Experimental

2.1 Materials and Methods

CAPE, 97% pure, CAF, NIC, INIC, gallic acid, p-coumaric acid, curcumin, isoniazide, theophylline, urea, ibuprofen (purity >98%) and taxifolin analytical standard were purchased from Sigma-Aldrich Company Ltd., UK. Ethanol (>99% pure) and acetonitrile (>99% pure) were also procured from Sigma-Aldrich Company Ltd., UK.

2.2. Synthesis of CAPE Cocrystals

A common procedure was used to screen all cofomers listed above (SII,ESI†) using microwave assisted cocrystallization technique for generation of cocrystals with CAPE. Equimolar amount of CAPE and the cofomer were mixed with ethanol to obtain 40 % w/w slurry in a 30 mL glass tube. The slurry was subjected to microwave irradiation in microwave reactor (Monowave 300, Anton Paar, Gmbh, Austria) to induce cocrystallization. The operating conditions were target temperature (80 °C), hold time (60 sec) followed by cooling to 40 °C, the solid product was dried and subjected to further characterization.

2.3. Powder X-ray diffraction (PXRD)

The microwave processed materials were screened for cocrystal formation on Bruker D8 advanced diffractometer (X-ray wavelength $\lambda = 0.154$ nm, source Cu-K α , voltage 40kV) with filament emission of 40 mA current. The samples were scanned from 2 to 30° 2 θ at a scan speed of 0.01° step width.

2.4. Differential scanning Calorimetry (DSC)

The microwave processed materials were subjected to thermal analysis using TA Instruments DSC 2000 differential scanning calorimeter. The samples were subjected to heating from 20°C to their respective melting temperature at rate of 10°C/ min in DSC cell under inert nitrogen environment. Standard aluminum pans were used.

2.5. Raman spectroscopy

Raman spectra were recorded using Renishaw In via Reflex bench top spectrometer coupled with 683 nm stabilized diode (Renishaw Plc., UK). A laser spot of diameter (footprint) 2 μm was obtained at specimen using a 100X objective lens. The spectra were collected using extended scanning mode over the wave number region of 3500–100 cm^{-1} . 10 scans were collected for each sample. Data analysis was performed using Galactic Grams AI 8.0 spectroscopy software (Thermo Electron Corporation).

2.6. X-Ray Crystallography

Single crystal X-ray data on CAPE-NIC cocrystal was collected on the Xcalibur Gemini EOS CCD diffractometer (Oxford Diffraction, Yarnton, UK) using Mo-K α , radiation at 298 K. Data reduction were performed using CrysAlisPro (version 1.171.33.55). OLEX2-1.0 and SHELX-TL 97 were used to solve and refine the reflections data. Non-hydrogen atoms were refined anisotropically. Hydrogen atoms on O and N were experimentally located in difference electron density maps. All C–H atoms were fixed geometrically using HFIX command in SHELX-TL. A check of the final CIF file using PLATON did not show any missed symmetry. X-Seed was used to prepare packing diagrams. The X-ray data are deposited with the Cambridge Crystallographic Data Centre (www.ccdc.cam.ac.uk) (CCDC No. 1478155).

2.7. Equilibrium Solubility measurements

CAPE and the cocrystal samples were individually added in small portions to 1 mL distilled water at room temperature (25 ± 0.5 °C) and stirred at 600 rpm. The addition of solids was stopped once they showed precipitation in the solvent. The systems were stirred for further

24 hrs to ensure equilibration of the solids with the solvent. The samples were filtered using 0.45 μm nylon filter. The filtrate was suitably diluted and subjected to High Performance Liquid Chromatographic (HPLC) analysis on Waters e-2695 system integrated with a PDA 2998 detector, Empower 3 software and Waters symmetry C18 column (4.6×250 mm, 5 μm) maintained at 25 ± 0.5 °C throughout study, see S12,ESI†. Amount of CAPE solubilized was calculated from calibration curve by plotting the known concentration at each dilution vs. the corresponding peak area.

2.8. *In vivo* pharmacokinetics

Male Wistar rats (n = 3 per group) weighing 200–250 g were purchased from National Toxicology Centre, Pune, India. CAPE and CAPE-NIC cocrystal samples were administered per oral at a dose of 100 mg CAPE per kg body weight. Blood was collected from retro-orbital plexus of rats at different time points as: 0, 5, 10, 15, 30, 45, 60, 120, 240, and 360 min. and analyzed for CAPE plasma concentration, see S13,ESI† for more details.

3. Results and Discussion

Data mining of the crystal structure database (CSD) in conjunction with the crystal engineering principles comprise the basic design elements for fabrication of multi-component cocrystals.³⁴⁻³⁹

Considering the nature of functional groups in CAPE molecule, coformers with complementary functional moieties were selected so as to form stable cocrystals. The primary functional groups in CAPE are 1,2-benzenediol and ester moieties. In literature, COOH, CONH₂ and pyridine functional groups have been reported to assemble with hydroxyl containing molecules.^{33, 37} Accordingly, CAPE was cocrystallized with GRAS listed coformers containing these functional groups. A complete list of all the coformers are listed in Table S11, ESI†.

3.1. Powder X-ray Diffraction

PXRD was employed as a fingerprint tool to examine the crystallinity and novelty of CAPE cocrystals. The experimental powder patterns of bulk materials of CAPE cocrystals and their respective individual components are shown in Figure 1a and Figure 1b. The new and unique diffraction peaks in the powder XRD patterns of cocrystal samples different from that of pure CAPE and coformers confirm cocrystallization.

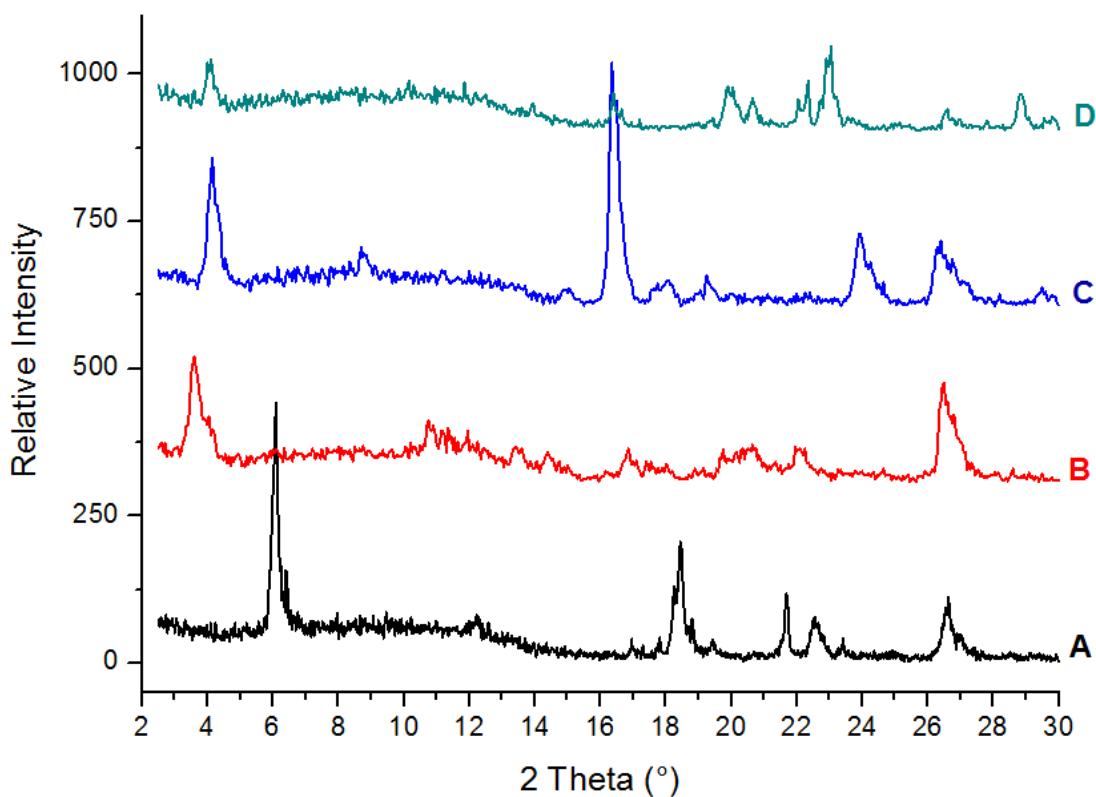


Figure 1a. Experimental powder diffraction patterns of A) pure CAPE; B) CAPE-CAF; C) CAPE-INIC and D) CAPE-NIC

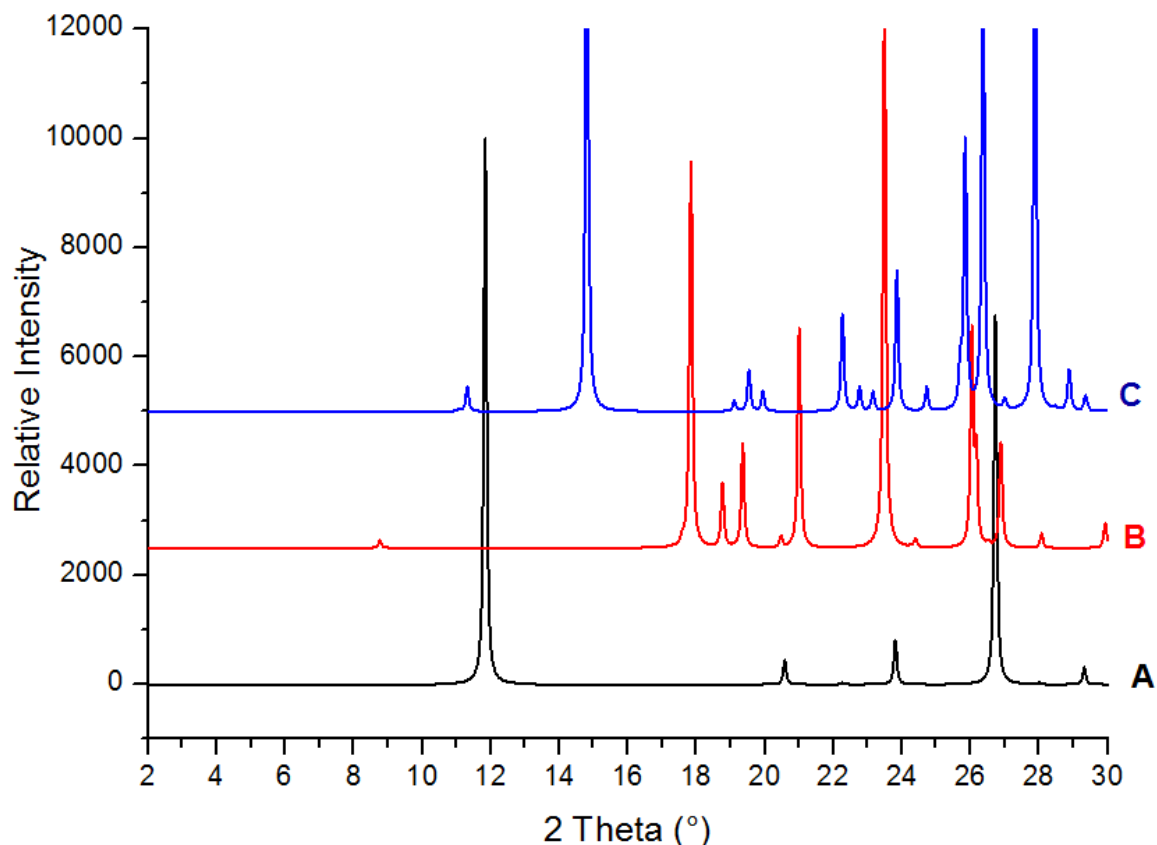


Figure 1b. Calculated powder diffraction patterns of pure A) caffeine; B) INIC and C) NIC

3.2. Differential Scanning Calorimetry

Differential scanning calorimetric analysis displayed unique thermal behavior and the phase purity of CAPE cocrystals. Interestingly, none of the cocrystals exhibited a melting point in between that of the corresponding individual components as observed in certain cocrystal systems³⁵ (Figure 2a and 2b). Instead, all the cocrystal phases exhibited lower melting point as compared to CAPE and the respective coformers. The cocrystal melting points showed a direct dependence on the coformer melting point, i.e. higher melting cocrystal was formed by a higher melting coformer (Table 1). Further, heat-cool-heat experiments on these cocrystals indicated that they did not undergo recrystallization on cooling, possibly the recrystallization event

followed a different cooling profile than the method adapted during our DSC analysis. (SI4, ESI†)

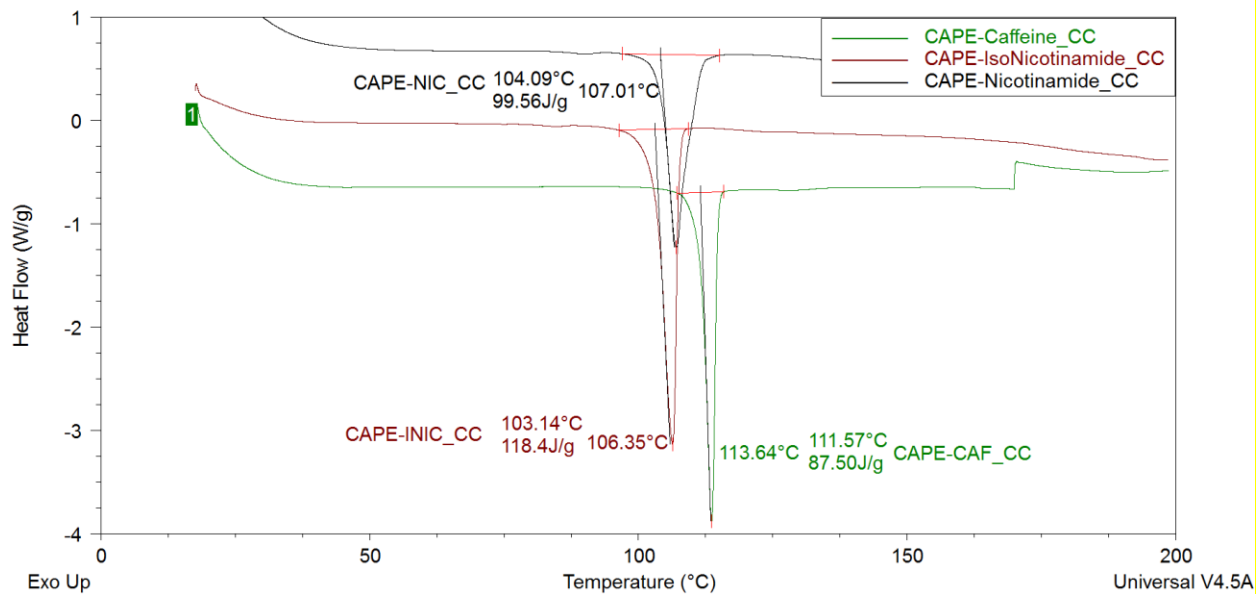


Figure 2a. DSC Heating curves for a) pure CAPE; b) CAPE-CAF; c) CAPE-INIC; d) CAPE-NIC; e) CAF f) INIC and g) NIC

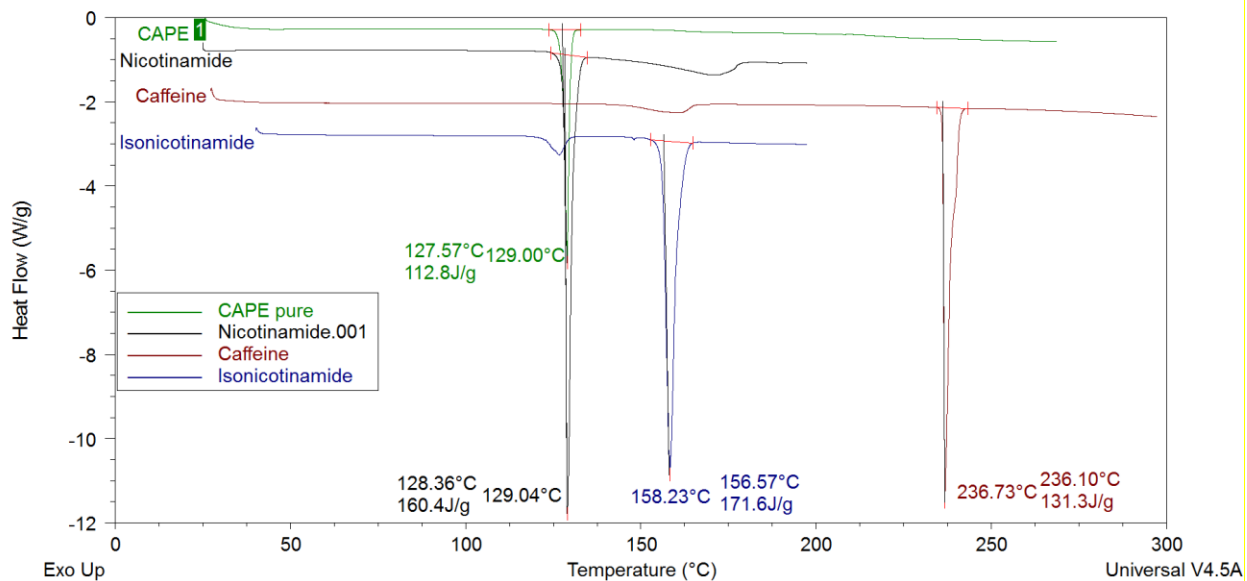


Figure 2b. DSC Heating curves for a) pure CAPE; b) CAF; c) INIC and d) NIC.

Table 1. DSC melting points of CAPE cocrystals and their conformers.

S. No.	CAPE cocrystal	Cocrystal melting Point (°C)	Coformer	Coformer melting Point (°C)
1	CAPE-NIC	107.01	Nicotinamide	129.04
2	CAPE-INIC	106.35	Isonicotinamide	158.23
3	CAPE-CAF	113.64	Caffeine	236.73

Melting point of CAPE is 129°C

3.3. Raman spectroscopy

CAPE and its cocrystals were characterized by Raman spectroscopy in order to ascertain the influence of solid state modification on the vibrational states of participating atoms and differentiate the novel crystalline phases from the starting materials. In the Raman spectrum of CAPE, the ester C=O stretch occurs at 1680.55 cm⁻¹, the asymmetric and symmetric C=C stretch occurs at 1598.7 and 1451.8 cm⁻¹ and the C-O stretch occurs at 1156.5 cm⁻¹. Similarly in the Raman spectrum of NIC, the N-H stretch occurs at 3368.9 cm⁻¹, the C=O at 1676.39 cm⁻¹ and C-O at 1159.3 cm⁻¹. On forming cocrystal, the amide C=O of NIC undergoes a red shift to 1634.7 cm⁻¹ indicating the enhanced single bond character of the C=O group on forming a hydrogen bond with the phenolic O-H of CAPE. The other cocrystals where crystal structures are not available currently, changes in their vibrational patterns may be explained through Raman spectrum. In pure INIC, the N-H stretch occurs at 3357.8 cm⁻¹ and the C=O at 1676.3 cm⁻¹. In the cocrystal, the amide C=O undergoes a blue shift to 1697.1 cm⁻¹ and C-O to 1163.4 cm⁻¹. In pure CAF, the C=O appears at 1695 cm⁻¹ which undergoes a red shift to 1687.5 cm⁻¹ in the

cocrystal. Thus, the Raman spectroscopy complement with other characterization techniques in establishing the formation of novel crystalline phases.

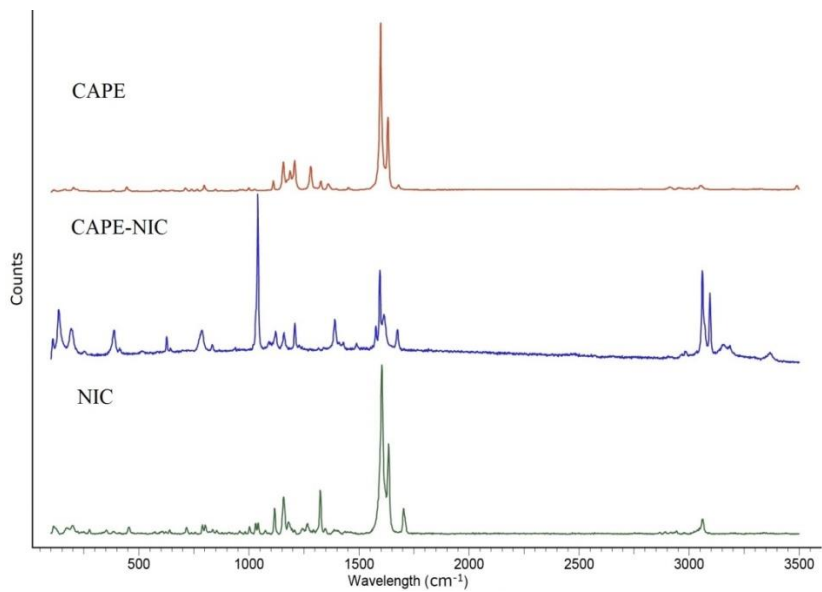


Figure 3. Raman spectrum of CAPE-NIC in comparison to its starting materials

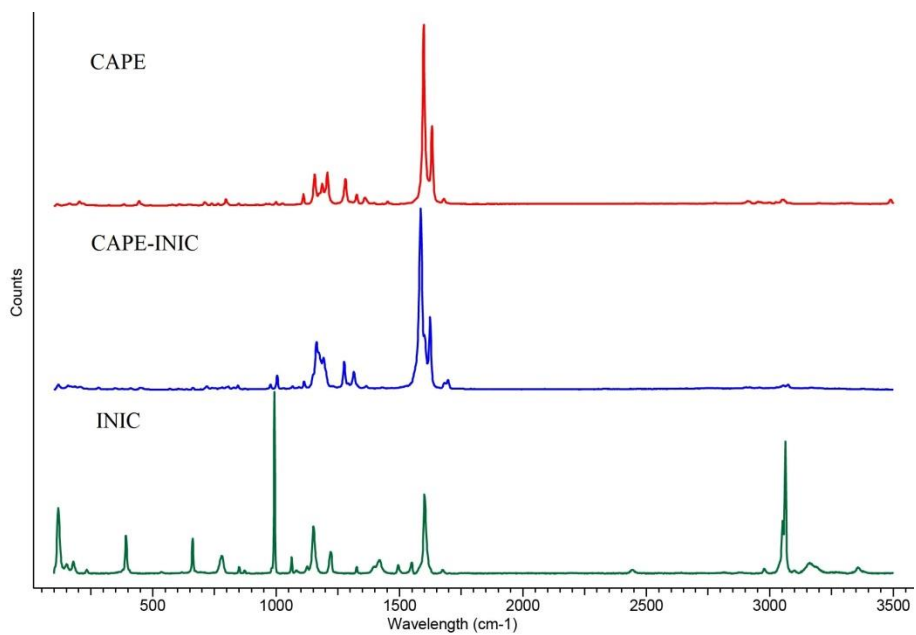


Figure 4. Raman spectrum of CAPE-INIC in comparison to its starting materials

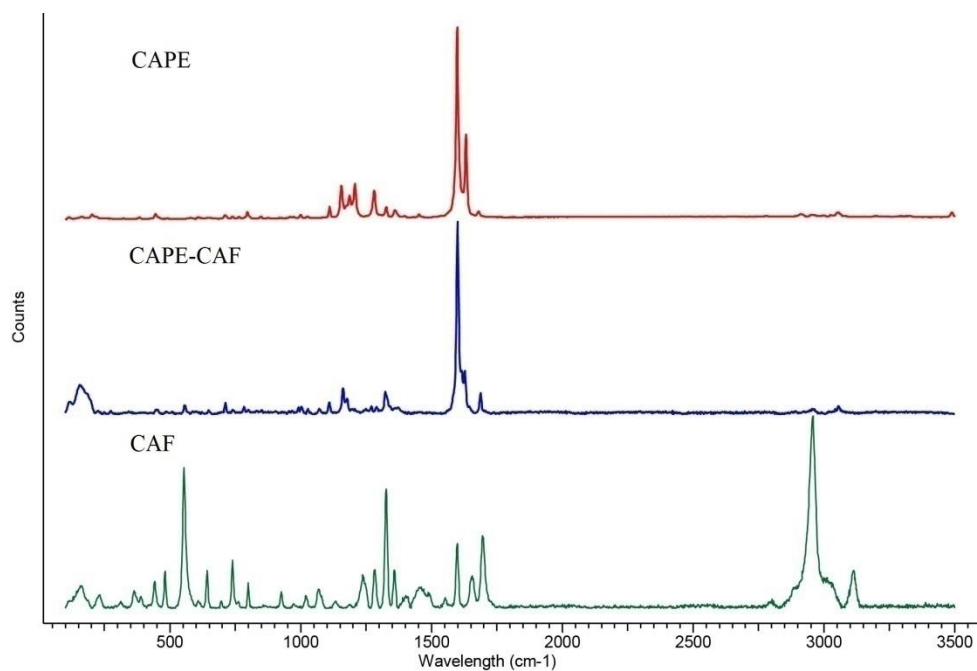


Figure 5. Raman spectrum of CAPE-CAF in comparison to its starting materials

3.4. Crystal Structure Analysis

CAPE-NIC cocrystal

Among the novel crystalline phases, crystal structure of CAPE-NIC was determined by SC X-ray crystallography. The structural parameters of CAPE-NIC are shown in Table 2 and the hydrogen bond parameters are listed in Table 3.

Table 2. Crystallographic Parameters of CAPE-NIC cocrystal.

Emp. Form.	C ₂₃ H ₂₂ N ₂ O ₅
Form. Wt.	406.43
Cryst. Syst.	Monoclinic
Sp. Gr.	<i>P2₁/c</i>
T (K)	298(2)
a (Å)	22.0039(15)
b (Å)	5.2382(4)
c (Å)	17.9644(16)
α (°)	90
β (°)	99.975(8)
γ (°)	90
Z	4
V (Å ³)	2039.3(3)
Total No. of Reflns.	6455
Unique Reflns.	3457
Obsd. Reflns.	2391
Parameters	287
R1	0.0500
wR2	0.1470
GOF	1.021

Table 3. Hydrogen bond distances and angles in CAPE-NIC cocrystal (neutron-normalized

D–H···A	D···A (Å)	H···A (Å)	D–H···A (°)	Symmetry code
CAPE–NIC (1:1)				
O1–H1···O5	2.790	1.96	148	$-x+1, +y-1/2, -z+1/2+1$
N2–H2B···O1	3.068	2.58	114	$-x+1, +y-1/2, -z+1/2+1$
N2–H2A···O5	3.088	2.29	150	$x, -1+y, z$
O2–H2···N3	2.708	1.74	164	$x, +y-1, +z+1$
C16–H16···O4	3.545	2.67	157	$-x+2, +y-1/2, -z+1/2+1$

N–H 1.030 Å, O–H 0.938 Å, and C–H 1.080 Å distances).

This 1:1 stoichiometric cocrystal crystallized in monoclinic $P2_1/c$ space group. A two-point heteromeric interaction between the 1,2-benzenediol moiety of CAPE and the amide of NIC (O1–H1···O5, 1.96Å, 148°; N2–H2B···O2, 2.26Å, 137°) is the primary H-bonding synthon in this cocrystal (Figure 6). Further, these heterodimers are connected through N–H···O (N2–H2B···O1 (phenolic oxygen), 2.58 Å, 114°; N2–H2A···O5 (amide oxygen), 2.29Å, 150°) H-bonds, extending them into the 2-dimensional space. The phenolic –OH (O2H2) further propagates this molecular assembly into the third dimension through O–H···N (O2–H2···N3 (pyridyl N), 1.74Å, 164°) H-bond with the adjacent pyridyl nitrogen. Apart from these strong hydrogen bonding synthons, weak C–H···O (C16–H16···O4, 2.67Å, 167°) and C–H··· π interactions ably assist in stabilizing the 3D packing in this cocrystal (Figure 7). The benzenediol-amide heterosynthon between CAPE and NIC is relatively rare interaction as compared to their respective homosynthons and competing heterosynthons. A CSD search for cocrystals with 1, 2-benzenediol and primary amide functional group lends credence to this statement (Table SI5,

ESI†). A CSD search (version 5.37, March 2016) with these functional groups on chemically different molecules resulted in 28 hits. Of these 24 crystal structures were stabilized by competing homosynthons (OH \cdots OH and amide-amide) heterosynthons such as acid-amide, OH-pyridine etc. Only four structures form the 1,2-benzenediol and amide heterosynthon. The predominance of crystal structures stabilized by competing heterosynthons indicates the diol-amide heterosynthon as a much weaker interaction. In the CAPE-NIC structure, the diol-amide heterosynthon was favored due to the absence of other functional groups and preferred over the competing homosynthons.

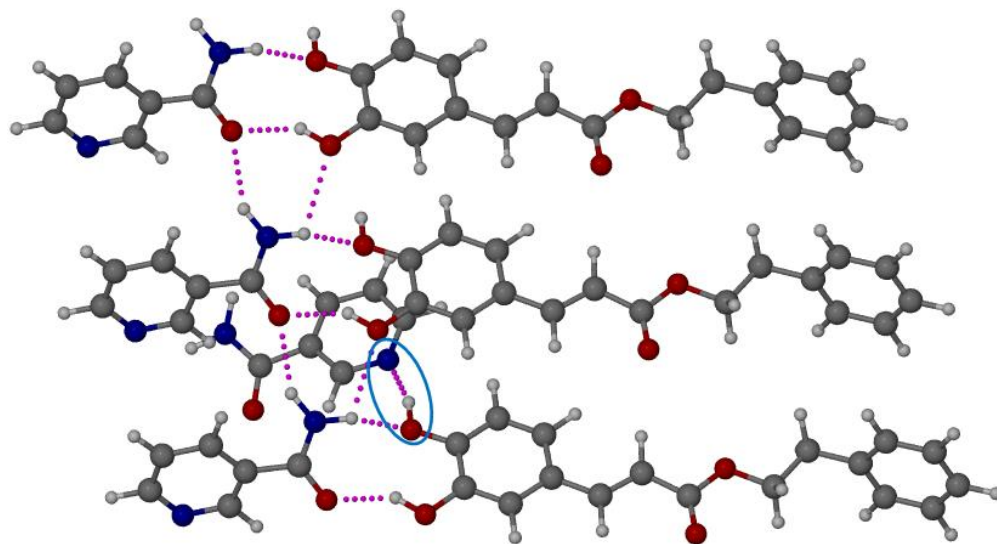


Figure 6. CAPE and NIC molecules connected through heteromeric two point synthon which are further held through N-H \cdots O H-bonds. The O-H \cdots N (pyridine) interaction is highlighted through a blue circle.

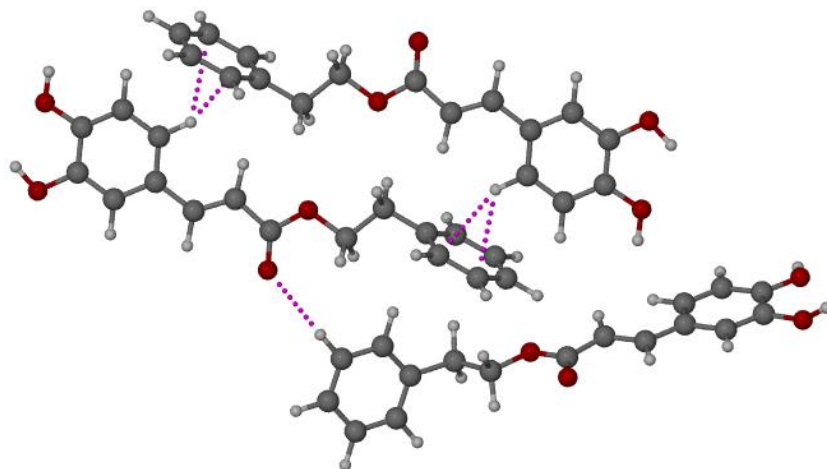


Figure 7. Weak C-H...O and C-H... π interactions further stabilize the CAPE-NIC crystal structure.

3.5. Equilibrium Solubility

The primary objective behind developing cocrystals of CAPE was to address its poor solubility, which significantly lowers its bioavailability limiting its efficacy. Our objective was based on the hypothesis that the high solubility cocrystals would alter the hydrogen bond patterns in the CAPE, which would improve its aqueous solubility envisaging enhancement in bioavailability. Equilibrium solubility experiments on CAPE and its cocrystals were performed in distilled water and the samples were analyzed by HPLC. The HPLC chromatograms demonstrated retention time (Rt) for standard solutions of CAPE, CAF, INIC and NIC to be 3.702 ± 0.02 , 3.123 ± 0.03 , 2.945 ± 0.02 and 3.006 ± 0.01 min, respectively and the same were observed for respective cocrystals (Figure SI6, ESI†). Solubility experiments, apart from confirming the poor aqueous solubility of CAPE (0.021 ± 0.0013 mg/mL), highlighted the advantage in forming cocrystals where the CAPE-CAF, CAPE-INIC and CAPE-NIC exhibited about 5.5, 7.5 and 17.7 times higher solubility as compared to pure CAPE (Table 4). Interestingly, the solubility profiles of

CAPE cocrystals are inversely related to their melting point. The lower melting CAPE-NIC exhibited higher solubility followed by CAPE-INIC and CAPE-CAF. Significant improvement in the aqueous solubility of CAPE-NIC may be ascribed to the higher solubility documented for nicotinamide in water.^{34,35} Further, the BFDH (Bravais, Friedel, Donnay and Harker) model hints (since this method is based purely on geometric considerations and completely neglects energetics, the result is mostly a qualitative view) at the morphology of CAPE-NIC cocrystal (Figure SI7, ESI†) where the hydrophilic -diol groups of CAPE project out of the major (100) face of the CAPE-NIC cocrystal structure burying the hydrophobic skeleton inside, enabling favorable interaction with the water molecules and thus increasing its solubility.⁴⁰

Table 4. Equilibrium solubility values of CAPE and its cocrystals.

Compound	Equilibrium Solubility (mg/mL)	X fold increment compared to CAPE	Melting point of cocrystal (°C)
CAPE	0.021 ± 0.0013	-	129
CAPE-CAF	0.115 ± 0.0011	5.5	113.48
CAPE-INIC	0.158 ± 0.0054	7.5	107.98
CAPE-NIC	0.371 ± 0.0052	17.7	106.67

3.6. *In vivo* pharmacokinetics

The poor water solubility of CAPE hampers its pharmacokinetic profile especially in terms of absorption upon oral administration. The present study was performed to trace the influence of cocrystallization of CAPE on its bioavailability. The 17 times improved solubility of CAPE-NIC

cocrystal, made it a lead entity to screen for its pharmacokinetic profile upon oral administration. Therefore emphasis was given on analyzing the absorption characteristics of the cocrystal in terms of plasma C_{max} and AUC values. No attempts were made to study detailed tissue distribution or *in vivo* side effects of the cocrystal samples. NIC is listed in the FDA's GRAS list and it is widely used and accepted as a food ingredient in many countries.⁴⁰ Also, its LD_{50} in rat is more than 4 gm per Kg per day.⁴¹ The amount of NIC used in the current study is much lower than its LD_{50} , thus suggesting its safety for oral administration to rat. The plasma concentration-time curves for CAPE in its pure form and CAPE from CAPE-NIC cocrystal are shown in Figure 8. The pharmacokinetic parameters for both are displayed in Table 5. Upon oral administration, CAPE showed C_{max} value of 35.2 ± 5.74 ng/mL at the end of 15 min (T_{max}) while CAPE-NIC cocrystal displayed C_{max} value of 75.1 ± 8.62 ng/mL at early 10 min (T_{max}). This suggests improved rate of absorption with administration of CAPE-NIC cocrystal. From the Figure 8 it is also evident that for every time point, CAPE concentrations in plasma of rats administered with CAPE-NIC cocrystal were remarkably higher than those administered with pure CAPE. After 360 min, the observed drug plasma concentrations with CAPE and CAPE-NIC cocrystal were 1.41 ± 0.48 ng/ml and 5.02 ± 2.60 ng/ml respectively. Further the $AUC_{(0-\infty)}$ values after oral administration of CAPE and CAPE-NIC cocrystal were found to be 2240 ± 136.71 ng.min/ml and 6736 ± 376.27 ng.min/ml respectively. Accordingly the CAPE-NIC cocrystal demonstrated high F_{REL} of 2.76 (bioavailability relative to that of parent drug). Moreover the elimination of drug appears to be slowed in case of CAPE-NIC cocrystal with $E_{T1/2}$ of 343 hr while that of 315 hr for CAPE. Clearly the results attested significant enhancement in systemic absorption of drug from CAPE-NIC cocrystal. Modulation of solubility of CAPE by cocrystallization with NIC

seems to be the most contributing factor in improving the pharmacokinetic profile of same. The NIC might have contributed to reduce first pass effect of liver enzymes on CAPE.¹¹

Table 5. *In vivo* pharmacokinetic parameters

Parameter	CAPE	CAPE-NIC
T _{max} (min)	15	10
C _{max}	35.2 ± 5.74	75.1 ± 8.62
AUC _{0-t}	1800 ± 148.26	4253 ± 266.38
AUC _(0-∞) (ng*min/mL)	2440 ± 136.71	6736 ± 376.27
FREL	1.00	2.76
A t _{1/2} (h)	8	1
D t _{1/2} (h)	61	22
E t _{1/2} (h)	315	343

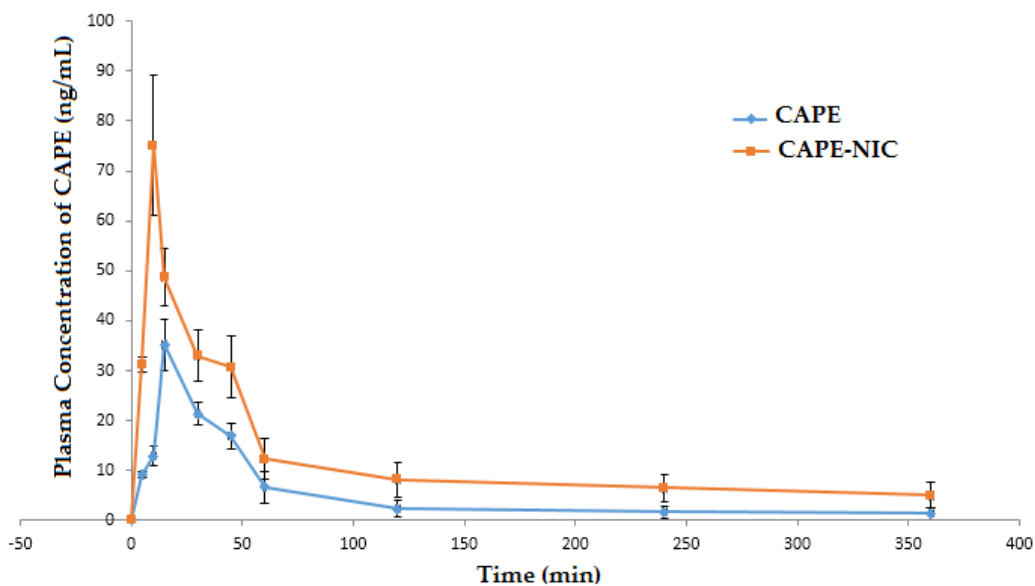


Figure 8. Pharmacokinetic profiles for CAPE and CAPE-NIC. (mean plasma concentration ± SD versus time).

4. Conclusion

The study confirms successful formation of novel crystalline phases for CAPE in the form CAPE-CAF, CAPE-INIC and CAPE-NIC cocrystals using microwave assisted cocrystallization technique. PXRD and DSC confirm synthesis and phase purity of CAPE-CAF, CAPE-INIC and CAPE-NIC cocrystals. Raman spectra of cocrystals complemented these results in conferring the formation of new crystalline phases of CAPE. Interestingly, the architecture of CAPE-NIC cocrystal as revealed by X-ray crystallography demonstrate stabilization of crystal structure by an uncommon 1,2-benzenediol-amide heterosynthon. Cocrystallization of CAPE with NIC evidently improved its aqueous solubility & pharmacokinetic profile thereby demonstrating 2.76 folds escalation in bioavailability.

Acknowledgement

We thank UKIERI: UK-India Education and Research Initiative (TPR26) and EPSRC (EP/J003360/1, EP/L027011/1) for providing financial support during this study. NRG thanks the CSIR for fellowship.

Supporting Information

Results about the screening of additional cofomers for the cocrystallization of CAPE along with the HPLC chromatograms and crystal structures have been provided as supporting information.

This material is available free of charge *via* the Internet at <http://pubs.acs.org>.

AUTHOR INFORMATION

Corresponding Author

1) Professor Anant Paradkar

Centre for Pharmaceutical Engineering Science, University of Bradford, Bradford, BD7 1DP, UK.

E-mail: A.Paradkar1@Bradford.ac.uk

2) Professor Ashwini Nangia

a) School of Chemistry, University of Hyderabad, Prof. C. R. Rao Road, Gachibowli, Hyderabad 500 046, India

ashwini.nangia@gmail.com

References:

1. Manach, C.; Scalbert, A.; Morand, C.; Remesy C.; Jiménez, L. *Am J Clin Nutr.***2004**, *79*, 727.
2. Manach, C.; Williamson, G.; Morand, C.; Scalbert A.; Remésy, C. *Am J Clin Nutr.***2005**, *81*, 230S.
3. Williamson G.; Manach, C. *Am J Clin Nutr.***2005**, *81*, 243S.
4. Perron N. R.; Brumaghim, J. L. *Cell Biochem Biophys.***2009**, *53*, 75.
5. Fresco, P.; Borges, F.; Diniz C.; Marques, M. *Med Res Rev.***2006**, *26*, 747.
6. Petti,S.; Scully, C. *Journal of dentistry.***2009**, *37*, 413.
7. Friedman, M. *Mol. Nutr.Food Res.***2007**, *51*, 116.
8. Yang, C. S.; Sang,S.; Lambert,J. D.; Lee, M. J. *Mol. Nutr. Food Res.***2008**, *52*, S139.
9. Hong, C.; Xie, Y.; Yao, Y.; Li, G.; Yuan X.; Shen, H. *Pharm. Res.***2015**, *32*, 47.
10. Sanphui, P.; Goud, N. R.; Khandavilli,U. R.; Nangia, A. *Cryst. Growth Des.***2011**, *11*, 4135.
11. Smith, A.J.; Kavuru, P.; Wojtas, L.; Zaworotko,M. J.; Shytle, R. D. *Mol. Pharm.***2011**, *8*, 1867.
12. Smith, J.; Kavuru, P.; Arora, K. K.; Kesani, S.; Tan, J.; Zaworotko,M. J.; Shytle, R. D. *Mol. Pharm.* **2013**, *10*, 2948.

13. Goud, N. R.; Suresh, K.; Sanphui, P.; Nangia, A. *Int. J. Pharm.* **2012**, *439*, 63.
14. Kavuru, P. Doctoral dissertation, University of South Florida, **2008**
15. Li, Konecke, S.; Harich, K.; Wegiel, L.; Taylor L. S.; Edgar, K. J. *Carbohydr Polym.* **2013**, *92*, 2033.
16. Tolba, M. F.; Azab, S. S.; Khalifa, A. E.; Abdel-Rahman, S. Z.; Abdel-Naim, A. B. *IUBMB life.* **2013**, *65*, 699.
17. Ozturk, G.; Ginis, Z.; Akyol, S.; Erden, G.; Gurel, A.; Akyol, O. *Eur Rev Med Pharmacol Sci.* **2012**, *16*, 2064.
18. Chen, Y.J.; Shiao, M.S.; Hsu, M.L.; Tsai, T.H.; Wang, S.Y. *J Agric Food Chem.* **2001**, *49*, 5615.
19. Michaluart, P.; Masferrer, J. L.; Carothers, A. M.; Subbaramaiah, K.; Zweifel, B. S.; Koboldt, C.; Mestre, J. R.; Grunberger, D.; Sacks, P. G.; Tanabe, T. *Cancer Res.* **1999**, *59*, 2347.
20. Sud'Ina, G.F.; Mirzoeva, O.K.; Pushkareva, M.A.; Korshunova, G.; Sumbatyan, N.V.; Varfolomeev, S.D. *FEBS letters.* **1993**, *329*, 21.
21. Nagaoka, T.; Banskota, A. H.; Tezuka, Y.; Saiki, I.; Kadota, S. *Bioorg Med Chem.* **2002**, *10*, 3351.
22. Wu, J.; Omene, C.; Karkoszka, J.; Bosland, M.; Eckard, J.; Klein, C. B.; Frenkel, K. *Cancer let.* **2011**, *308*, 43.

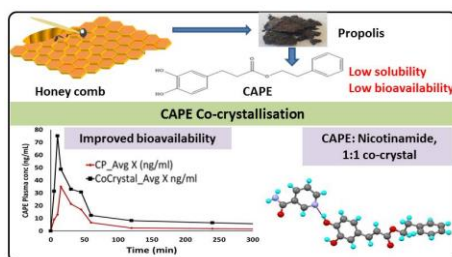
23. Lee, Y.T.; Don, M.J.; Hung, P.S.; Shen, Y.C.; Lo, Y.S.; Chang, K.W.; Chen, C.F.; Ho, L. *K. Cancer let.* **2005**, *223*, 19.
24. Demestre, M.; Messerli, S.; Celli, N.; Shahhossini, M.; Kluwe, L.; Mautner, V.; Maruta, H. *Phytother Res.* **2009**, *23*, 226.
25. Ceschel, G.; Maffei, P.; Sforzini, A.; Borgia, S. L.; Yasin, A.; Ronchi, C. *Fitoterapia.* **2002**, *73*, S44.
26. Wang, X.; Bowman, P. D.; Kerwin, S. M.; Stavchansky, S. *Biomed Chromatogr.* **2007**, *21*, 343.
27. Celli, N.; Mariani, B.; Dragani, L. K.; Murzilli, S.; Rossi, C.; Rotilio, D. J. *Chromatogr. B.* **2004**, *810*, 129.
28. Xian-ling, N.; Xiao, M. *JCPS.* **2011**, 201, 20.
29. Ketabforoosh, S. H. E.; Amini, M.; Vosooghi, M.; Shafiee, A.; Azizi, E.; Kobarfard, F. *IJPR.* **2013**, *12*, 705.
30. Shi, H.; Xie, D.; Yang R.; Cheng, Y. *J Agric Food Chem.* **2014**, *62*, 5046.
31. Murtaza, G.; Karim, S.; Akram, M. R.; Khan, S. A.; Azhar, S.; Mumtaz, A.; Bin Asad, M. H. H. *BioMed Res Int.* **2014**, Article ID 145342: 1-9.
32. Sopheak, S.; Lobkowsky E. B.; Lewis, B. A. *Notes.* **2001**, *49*, 236.
33. Pagire, S.; Korde, S.; Ambardekar, R.; Deshmukh, S.; Dash R. C.; Dhumal R.; A. Paradkar, *CrystEngComm.* **2013**, *15*, 3705.

34. Desiraju G. R. *Angew. Chem. Int. Ed. Engl.* **1995**, *34*, 2311.
35. Walsh, R. D. B.; Bradner, M. W.; Fleischman, S.; Morales, L. A.; Moulton, B.; Rodriguez-Hornedo, N.; Zaworotko, M. J. *Chem Commun.* **2003**, 186.
36. Etter, M. C. *Acc. Chem. Res.* **1990**, *23*, 120.
37. Etter, M. C. *J. Phys. Chem.* **1991**, *95*, 4601.
38. Schultheiss, N.; Newman, A. *Cryst. Growth Des.* **2009**, *9*, 2950.
39. Goud, N. R.; Gangavaram, S.; Suresh, K.; Pal, S.; Manjunatha, S. G.; Nambiar S.; Nangia, A. *J. Pharm. Sci.* **2012**, *101*, 664.
40. Francesco, P., *J Mol Str*, **2013**, *1032*, 147.
41. CFR – Code of Federal Regulations Title 21, Volume 3, April 2015.
<https://www.accessdata.fda.gov/scripts/cdrh/cfdocs/cfcfr/CFRSearch.cfm?fr=184.1535>
42. FDA - Select Committee on GRAS Substances (SCOGS) Opinion: Niacinamide (nicotinamide).
<http://www.fda.gov/Food/IngredientsPackagingLabeling/GRAS/SCOGS/ucm260908.htm>

Insert Table of Contents Graphic and Synopsis Here

Tracing the architecture of Caffeic acid phenethyl ester cocrystals: Studies on crystal structure, solubility and bioavailability implications

Sameer Ketkar[†], Sudhir K.Pagire[‡], N. Rajesh Goud[‡], KakasahebMahadik[‡], AshwiniNangia^{‡,¶*} and AnantParadkar^{‡*}



Caffeic Acid Phenethyl Ester (CAPE) is a poorly water-soluble antioxidant with range of therapeutic applications. It is a constituent of propolis, a resinous material collected by honeybees. In this study, we report significant improvement in solubility and bioavailability of CAPE by forming a novel cocrystal of CAPE with nicotinamide as cofomer. The cocrystal has shown 2.76 fold improvement in bioavailability of CAPE.

Supporting Information

Tracing the architecture of Caffeic acid phenethyl ester cocrystals:
Studies on crystal structure, solubility and bioavailability implications

Sameer Ketkar[†], *Sudhir K Pagire*[‡], *N. Rajesh Goud*[‡], *Kakasaheb Mahadik*[†], *Ashwini Nangia*^{‡,¶*} and *Anant Paradkar*^{‡*}

[†] Centre for Advanced Research in Pharmaceutical Sciences, Poona College of Pharmacy, Bharati Vidyapeeth University, Pune-411038, India.

[‡] Centre for Pharmaceutical Engineering Science, University of Bradford, Bradford, BD7 1DP, UK.

[‡] School of Chemistry, University of Hyderabad, Prof. C. R. Rao Road, Gachibowli, Hyderabad, 500 046, India.

[¶] CSIR-National Chemical Laboratory, Dr. Homi Bhabha Road, Pune 411 008, India.

Table of Content

SI1	Cofomers screened for cocrystallization with CAPE (1:1)
SI2	Details of HPLC method for CAPE analysis
SI3	Details of in vivo pharmacokinetic study
SI4	Differential Scanning Calorimetry (DCS), Heat-Cool-Heat study for CAPE-NIC, CAPE-INIC and CAPE-CAF co-crystals
SI5	Refcodes with 1,2-benzenediol and amide functional groups in the same crystal structure.
SI6	HPLC Chromatograms of CAPE and its cocrystals.
SI7	BDFH morphology crystals (calculated)

SII. Coformers screened for cocrystallization with CAPE (1:1).

No.	Coformer	Melting point (°C)	Solvent (60% w/v)	Observations	Inference
1	Caffeine (CAF)	235-238	Ethanol	i) DSC thermogram showed melting endotherm at 113.48°C. ii) PXRD showed distinct peak at 2θ value 3.5.	Formation of CAPE:CAF cocrystal was evident (however diffraction quality single crystal was not produced)
2	Nicotinamide (NIC)	130-131	Ethanol	i) DSC thermogram showed melting endotherm at 106.67°C. ii) PXRD showed distinct peak at 2θ value 4.6.	Formation of CAPE:NIC cocrystal was evident Also diffraction quality single crystal was produced.
3.	Isonicotinamide (INIC)	155-157	Ethanol	i) DSC thermogram showed melting endotherm at 107.98 °C. ii) PXRD showed distinct peak at 2θ value 4.6.	Formation of CAPE:CAF cocrystal was evident. (however diffraction quality single crystal was not produced)
4.	Gallic acid	257-258	Ethanol	DSC thermogram showed endotherm peaks at 113.8, 117.14 and 275.6 °C.	No cocrystal was produced.

No.	Coformer	Melting point (°C)	Solvent (60% w/v)	Observations	Inference
			Methanol	DSC thermogram showed sharp endotherm peaks at 127.88 °C and degradation above 225 °C	No cocrystal was produced.
			Acetone	DSC thermogram showed sharp endotherm peak 128.23°C	No cocrystal was produced.
			Ethyl acetate	DSC thermogram showed sharp endotherm peak 128.23°C	No cocrystal was produced.
5.	p-Coumaric acid	210-212	Ethanol	DSC thermogram showed endotherm peak at 126.84 °C and degradation above 190 °C.	No cocrystal was produced.
	p-Coumaric acid		Methanol	DSC thermogram showed endotherm peak at 125.45 °C and degradation above 190 °C.	No cocrystal was produced.
	p-Coumaric acid		Acetone	DSC thermogram showed endotherm peak at 126.50 °C and degradation above 194 °C.	No cocrystal was produced.
	p-Coumaric acid		Ethyl acetate	DSC thermogram showed endotherm peak at 125.80 °C and degradation above 195 °C.	No cocrystal was produced.

No.	Coformer	Melting point (°C)	Solvent (60% w/v)	Observations	Inference
6.	Curcumin	182-184	Ethanol	DSC thermogram showed endotherm peak at 122.47 °C.	No cocrystal was produced.
			Methanol	DSC thermogram showed endotherm peak at 122.47 °C.	No cocrystal was produced.
			Ethyl acetate	DSC thermogram showed endotherm peak at 122.47 °C.	No cocrystal was produced.
7.	Isoniazid	171-172	Ethanol	DSC thermogram showed endotherm peak at 101.47 °C.	No cocrystal was produced.
8.	Theophylline	273-274	Ethanol	DSC thermogram showed endotherm peak at 117.30 °C.	No cocrystal was produced.
9.	Urea	132-134	Ethanol	DSC thermogram showed endotherm peak at 99.95 and 133.14 °C.	No cocrystal was produced.
10.	Ibuprofen	75-76	Ethanol	DSC thermogram showed endotherm peak at 74 and 121.69 °C.	No cocrystal was produced.

SI2. Details of HPLC method for CAPE analysis

Waters e-2695 HPLC system integrated with a PDA 2998 detector, Empower 3 software and Waters symmetry C18 column (4.6 × 250 mm, 5 μm) maintained at 25 ± 0.5 °C was used. Elution was carried out using mobile phase methanol: acetonitrile (50: 50 v/v) in an isocratic method at a flow rate of 1 mL/min.¹ CAPE detection was done at 246 nm. Each experiment was performed in triplicates.

SI3. Details of in vivo pharmacokinetic study

The experiment protocol (CPCSEA/40/12), was approved by Institutional Animal Ethical Committee (IAEC) constituted as per guidelines of the Committee for Purpose of Control and Supervision of Experiments on Animals Government of India. The animals were housed under standard conditions of temperature (24 ± 1 °C), relative humidity (55 ± 10%) and 12 hrs light/dark cycles during said period. Animals had free access to standard pellet diet, filtered water ad libitum and were acclimatized for a period of one week prior to study. The animals were starved overnight prior to the study. Vegetable oil was used as gavage vehicle as all the crystal forms were found insoluble in it. The blood samples were mixed thoroughly with di-sodium EDTA to prevent clotting and centrifuged at 10,000 rpm for 15 min at 4 °C. The separated plasma was transferred to pre-labeled tubes containing sodium fluoride (0.25%) and acetate buffer (0.1M) to ensure the integrity of CAPE during storage at -80 °C till analysis.^{2,3}

Quantification of CAPE in Rat plasma

Standard solutions of CAPE and internal standard (IS), Taxifolin were prepared by dissolving each 10 mg in methanol 10 ml. The working standard solutions were prepared by diluting the stock solutions with mobile phase and spiked into the blank plasma to produce plasma

standards. The plasma samples were analysed for CAPE content by HPLC as per reported method with minor modifications. Briefly, 200 μ l of each plasma sample was mixed with 100 μ l of IS (100 μ g/ml) and extracted with 600 μ l of ethyl acetate by vortexing for 15 min. The collected supernatant phase from both extractions was dried under nitrogen flow at room temperature. The dried residues each were reconstituted with 200 μ l acetonitrile, filtered through 0.45 μ m nylon syringe and subjected to HPLC analysis for determination of CAPE content using Waters e-2695 system integrated with a PDA 2998 detector, Empower 3 software and Waters symmetry C18 column (4.6 \times 250 mm, 5 μ m) maintained at 25 \pm 0.5 $^{\circ}$ C throughout study. Elution was carried out with flow rate of 0.5 mL/min at ambient temperature. The solvents comprised acetonitrile (solvent A) and water (solvent B) both with 0.5% formic acid mixed using linear gradient system: initial 85% B, 25% B in 3 min, 10% B in 10 min, 0 % B in 15 min followed by isocratic 85% B held constant till 45 min. Detection was performed between 200 to 400 nm and chromatograms were extracted at 328 nm. The concentration range of the standard curve was 2 to 20 ng/mL of CAPE.

Data analysis

Pharmacokinetic parameters were calculated for the set of data by two compartment analysis using WinNonLin version 4.0 (Pharsight, Mountain View, CA,).

SI4. Differential Scanning Calorimetry (DCS), Heat-Cool-Heat study for CAPE-NIC, CAPE-INIC and CAPE-CAF co-crystals.

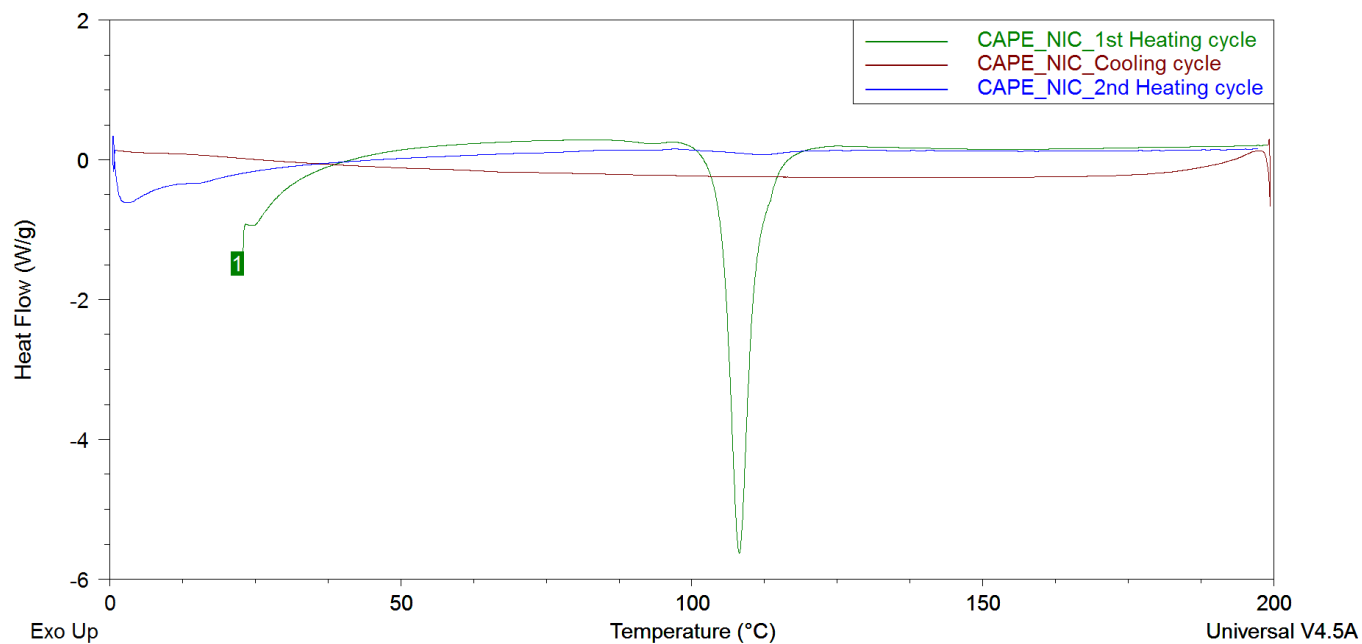


Figure SI4.A. DSC thermogram of CAPE-NIC co-crystal, Heat-Cool-Heat cycle.

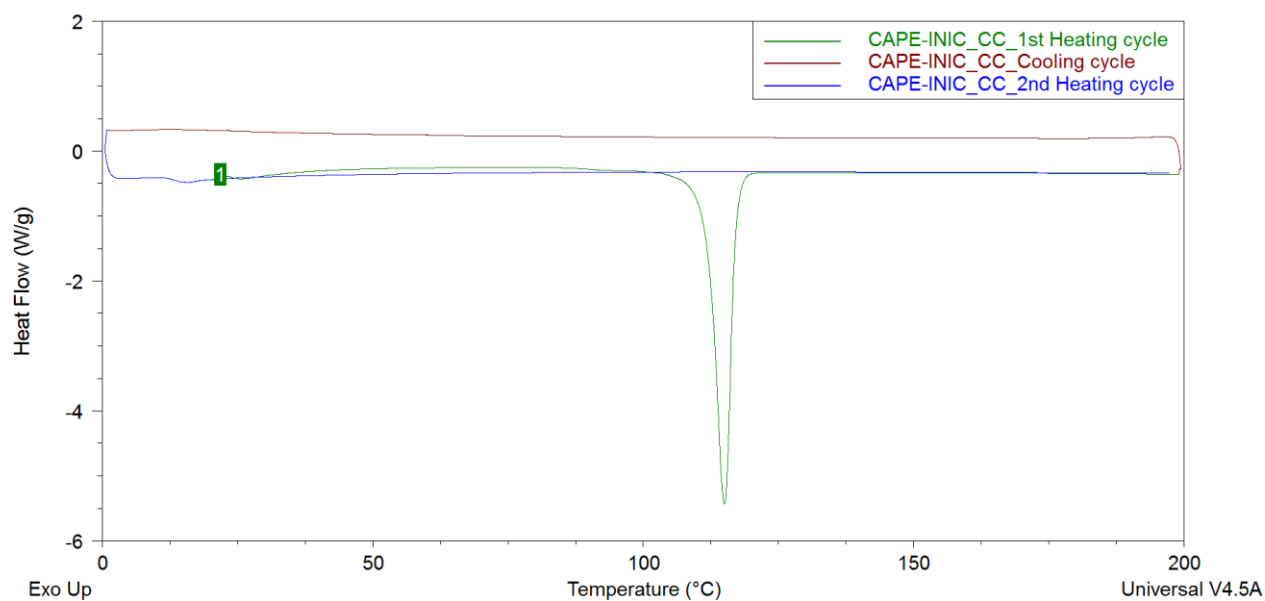


Figure SI4.B. DSC thermogram of CAPE-INIC co-crystal, Heat-Cool-Heat cycle.

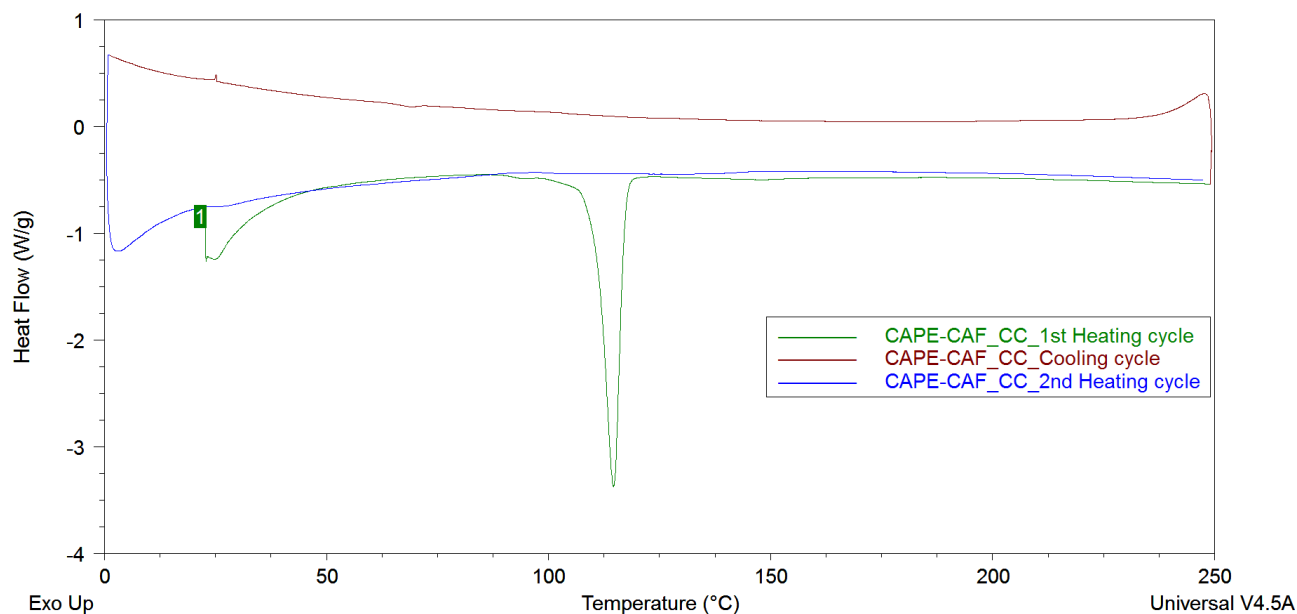


Figure SI4.C. DSC thermogram of CAPE-CAF co-crystal, Heat-Cool-Heat cycle.

SI5. Refcodes with 1,2-benzenediol and amide functional groups in the same crystal structure.

EVIJUO	FIXROV	GAZWUB	HEDRAL	HEDREP
HEDRIT	HEDROZ	HUMJII	MUPMOA	MUPNAN
MUPNUH	MUPPAP	NAXHOL	PEFGEO	PEFGEO01
PEFGEO02	PEFGEO03	PEFGIS	REBXIH	VEQTIW
ZEBXEL	ZEBXIP	ZEBXOV	ZEBXUB	ZIKNOY
ZIKPAM	ZIKPUG			

The reffcodes marked in **RED** represent crystal structures with benzene diol and amide heterosynthon

The reffcodes marked in **BLUE** represent crystal structures with competing homosynthons such as amide-amide, OH-OH etc

The reffcodes marked in **BLACK** represent crystal structures with other heterosynthons such as acid-amide, amide-pyridine etc.

SI6. HPLC Chromatograms of CAPE and its cocrystals.

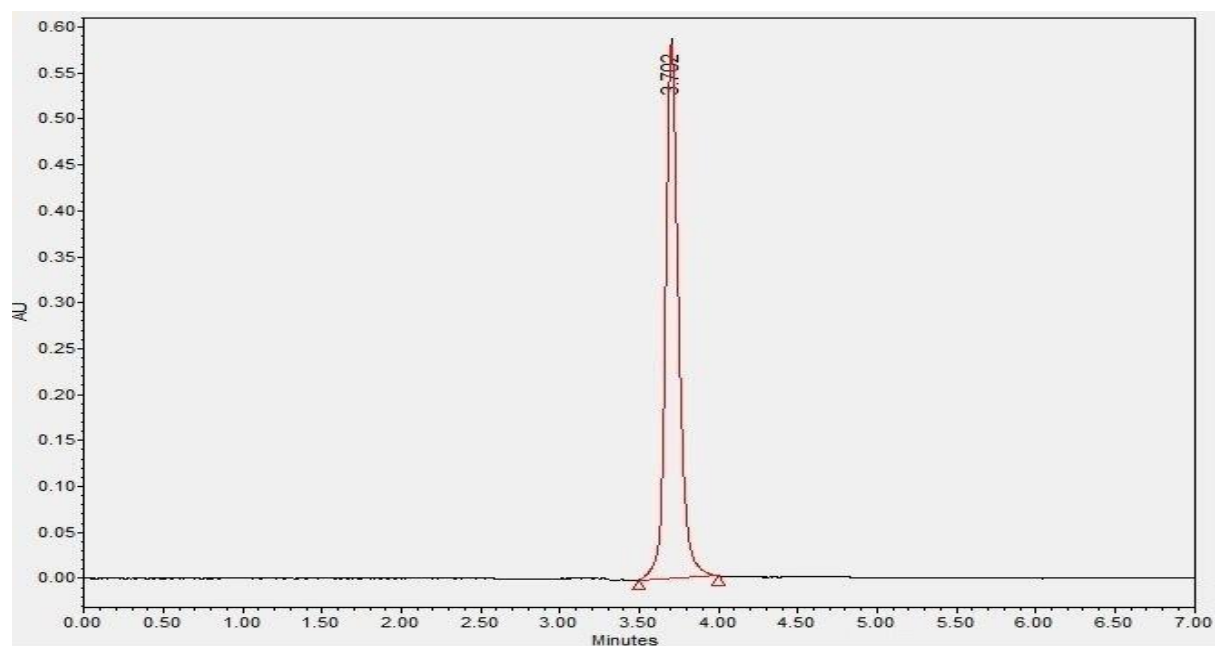


Figure SI6.A. Representative HPLC chromatogram of CAPE.

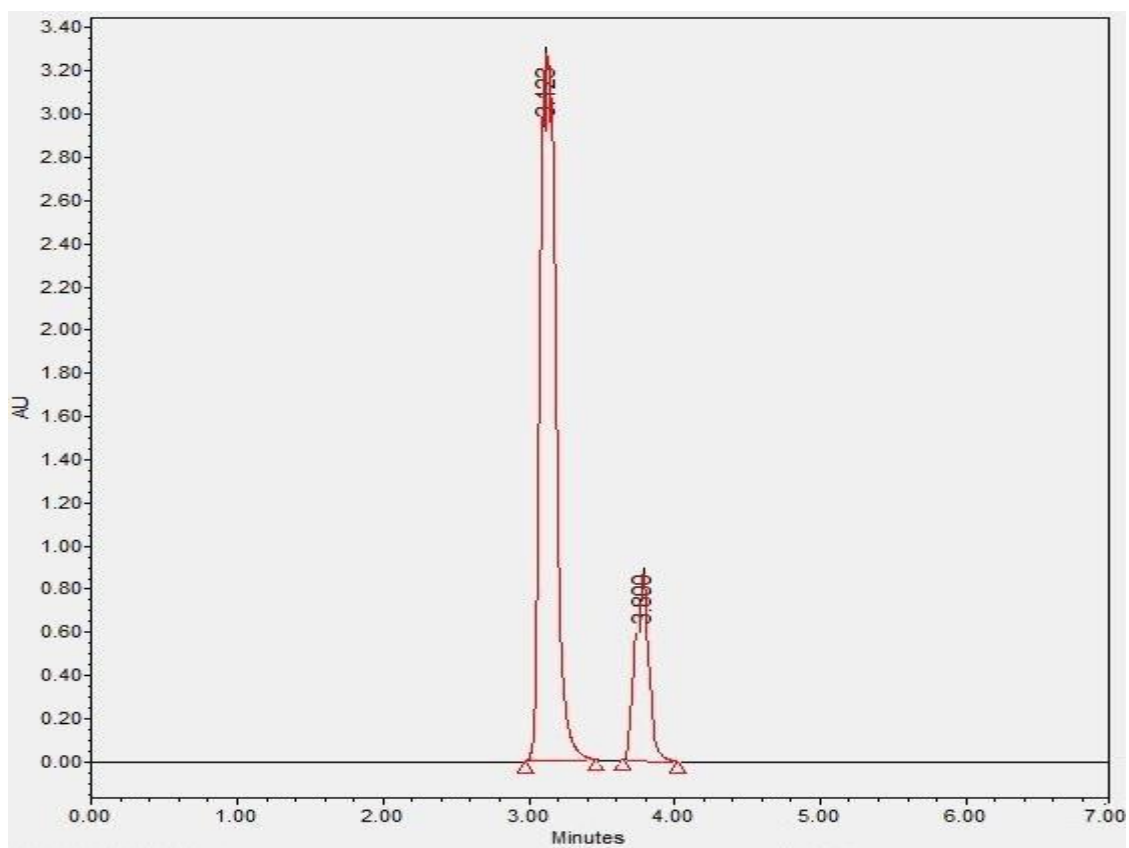


Figure SI6.B. Chromatogram for CAPE-CAF. The chromatogram depicts elution at 3.123 min for CAF and 3.80 min for CAPE.

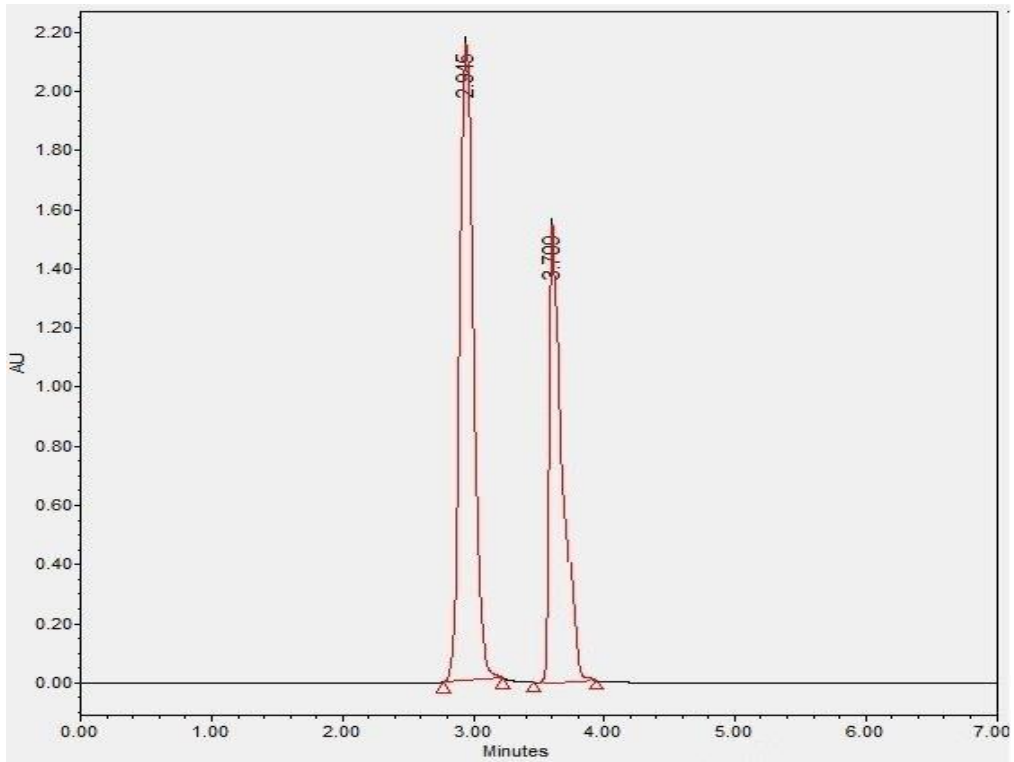


Figure SI6.C. Chromatogram for CAPE-INIC. The chromatogram depicts elution at 2.915 min for INIC and 3.70 min for CAPE.

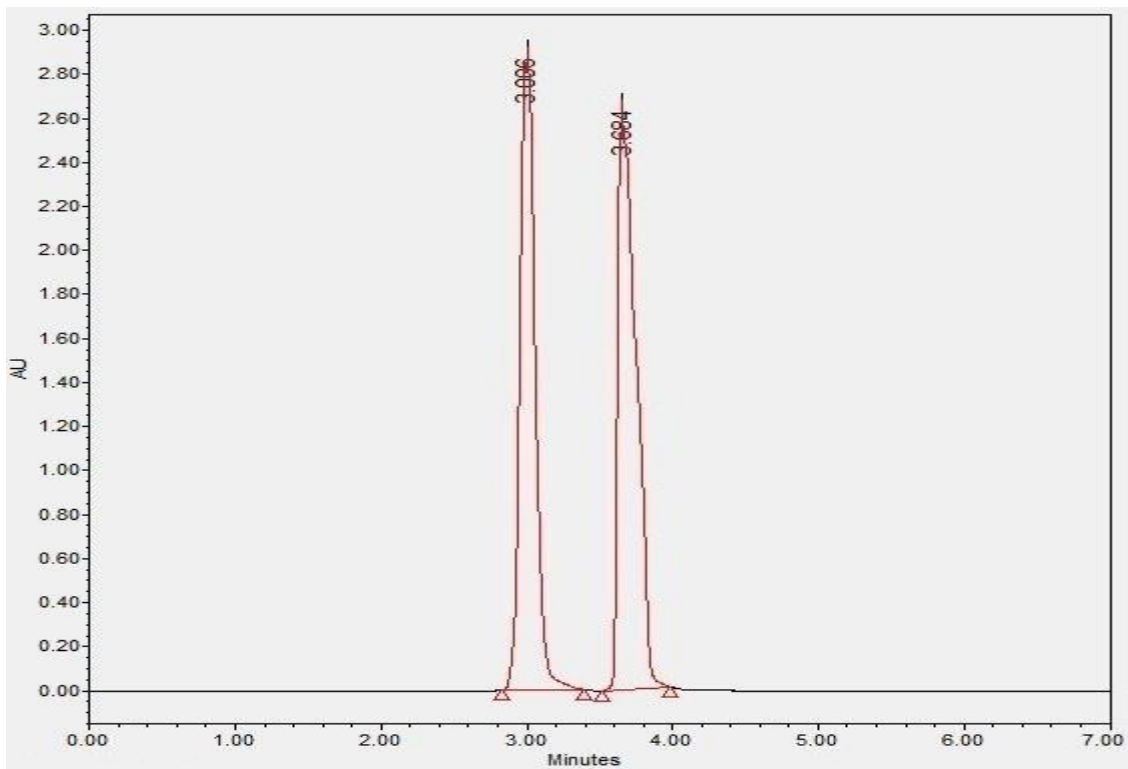


Figure SI6.D. Chromatogram for CAPE-NIC. The chromatogram depicts elution at 3.006 min for NIC and 3.684 min for CAPE.

SI7. BFDH morphology crystals (calculated)

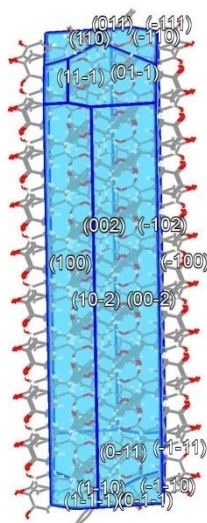


Figure SI7.A. BFDH model of CAPE-NIC showing the projected diol groups long the major (100) face. (Projected parallel to the (100) face)

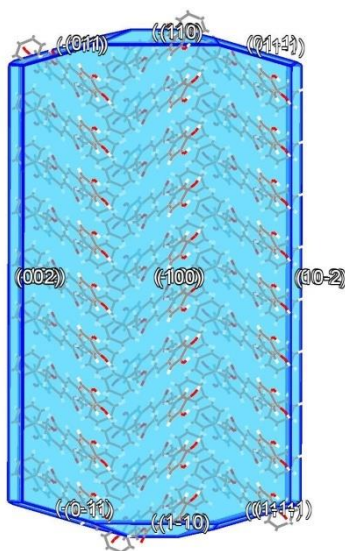


Figure SI7.B. BFDH model of CAPE-NIC showing the projected diol groups long the major (100) face. (Projected perpendicular to the (100) face)

References

1. Ceschel, G.; Maffei, P.; Sforzini, A.; Borgia, S. L.; Yasin, A.; Ronchi, C. *Fitoterapia*. **2002**, *73*, S44.
2. Wang, X.; Bowman, P. D.; Kerwin, S. M.; Stavchansky, S. *Biomed Chromatogr*. **2007**, *21*, 343.
3. Celli, N.; Mariani, B.; Dragani, L. K.; Murzilli, S.; Rossi, C.; Rotilio, D. J. *Chromatogr. B*. **2004**, *810*, 129.